HOLOGRAPHIC TECHNIQUES FOR ASYMPTOTICALLY-FREE GAUGE THEORIES

U. GURSOY[1], E. KIRITSIS[1,2], L. MAZZANTI[1], F. NITTI[1]

[1] *CPHT,Ecole Polytechnique, 91128, Palaiseau, FRANCE, (UMR du CNRS 7644)*
[2] *Department of Physics, University of Crete, 71003 Heraklion, GREECE*

Novel techniques based on holographic ideas are tried on the prototype strongly coupled gauge theory: QCD The ideas are developed and a well motivated phenomenological model (Improved Holographic QCD) is presented and compared to various non-perturbative regimes, both at zero and finite temperature.

1 Introduction

Strongly coupled gauge theories are omnipresent in theoretical physics, and have been forced experimentally upon us with the realization that the strong interactions are best described by an asymptotically free SU(3) gauge theory. The gauge coupling is weak at large energies and perturbation theory is applicable. However it is strong at low energy and almost all realistic observables contain parts that are sensitive to strongly coupled physics.

Beyond QCD, theorists have argued that strongly coupled gauge theories can play an important role in the physics beyond the standard model. We will mention here two such incarnations. The first concerns a strongly coupled gauge theory that is responsible for producing a composite Higgs that will break the electroweak symmetry at lower energies, [1]. Such classes of theories come under the name of 'technicolor" and although their popularity had its ups and downs, they are reanalyzed currently due to the use of novel non-perturbative holographic tools.

The second example concerns strong coupling dynamics that can trigger supersymmetry

breaking in a hidden sector. This supersymmetry breaking is expected to be transferred to the Supersymmetric SM sector either via universal interactions (gravity) or via gauge gauge interactions (gauge mediation). We should also mention that in theories beyond the SM, and especially in string theory vacua, strongly coupled hidden sectors are generic [2] and if their associated scales are in the TeV region they might produce signals at LHC.

Various techniques have been developed to deal with the strong coupling problem of gauge theories. The most straightforward one, is numerical evaluation of the quantities of interest on a computer. This is the lattice approach that has been applied mostly to QCD, with considerable success. The lattice approach after 30 years is a mature discipline that has however its limitations, that basically translate into limitations of computing power. Despite the success of computational approaches, several interesting QCD observables remain out of reach, or cannot be computed to the required accuracy (examples are transport coefficients at finite temperature, relevant for recent heavy ion data from RHIC, or the physics at finite baryon number density and chemical potential)

A different theoretical approach was postulated by 't Hooft in 1974, in order to generate a different perturbative expansion of strongly-coupled gauge theories. This is known as the large-N expansion where N is the number of colors. Although it turned out that it was not possible to calculate even the leading approximation in this expansion for 4d gauge theories, several important properties were uncovered [4]: (a) The perturbative expansion in powers of 1/N has the structure of a string theory with string coupling constant $g_s \sim 1/N$. (b) The gauge invariant QCD bound states, namely glueballs and mesons are non-interacting with O(1) masses, to leading order. Their widths vanish as $1/N^2$ for glueballs and 1/N for mesons. (c) Baryons are heavy, with masses N, and behave as solitonic objects. Theorists have attempted to construct this string theory in four dimensions, but existing experience with string theories did not suggest optimism in this direction.

A new twist to the quest of the string theory underlying a strongly coupled gauge theory came with the realization [5] that for such a gauge theory string should propagate in more than 4 dimensions. In a much more symmetric relative of QCD, namely $\mathcal{N}$=4 superconformal SU(N) gauge theory, the dual string theory turned-out to be a type IIB string propagating in a ten-dimensional spacetime of the form $AdS_5 \times S^5$. In particular the fifth (radial) dimension of AdS_5 provided the holographic dimension that somehow captured the RG scale of the four-dimensional gauge theory that was defined on the AdS_5 boundary. This duality turned out to be a weak-strong coupling duality in the following sense: The gauge theory, that is exactly conformally invariant, has two dimensionless parameters: the number of colors N that we take large, and the 't Hooft coupling $\lambda \equiv g^2_{YM}N$ that we keep fixed in the large-N limit. When $\lambda \ll 1$ one can use perturbation theory, and the relevant leading order diagrams are the planar diagrams. When $\lambda \gg 1$ perturbative techniques are of no use even as $N \to \infty$. On the other hand, the dual string theory is propagating on a manifold with curvature scale $1/\ell^2$, whose relation to the string length ℓ_s involves the 't Hooft coupling: $\ell^2 = \sqrt{\lambda}\, \ell_s^2$. Moreover as the YM gauge coupling constant is given by $g^2_{YM} \sim g_s$, the string coupling constant in the large-N limit is given by $g_s \sim \frac{\lambda}{N}$ and for fixed λ it is $\mathcal{O}(1/N)$. Therefore, at large-N and large 't Hooft coupling, $\lambda \to \infty$, the theory is described by a string that moves on a weakly curved ten-dimensional manifold, and can therefore approximated by the dynamics of its zero modes: the strongly coupled large-N sYM theory is equivalent to type IIB supergravity on the $AdS_5 \times S^5$ background.

Since [5] there has been a flurry of attempts to devise such correspondences for gauge theories with less supersymmetry with the obvious final goal: QCD. Several interesting string duals with a QCD-like low-lying spectrum and confining IR physics were proposed [6]. Although such theories reproduced the qualitative features of IR QCD dynamics, they contain Kaluza-Klein modes, not expected in QCD, with KK masses of the same order as the dynamical scale of the gauge theory. Above this scale, the theories deviate from QCD.

A different and more phenomenological approach was in the meantime developed and is now known as AdS/QCD. The original idea was formulated in [7] and it was successfully applied to the meson sector in [8]. The bulk gravitational background consists of a slice of AdS_5, and a constant dilaton. There is a UV and an IR cutoff. Moreover, the confining IR physics is imposed by boundary conditions at the IR boundary. This approach, although crude, has been partly successful in studying meson physics, despite the fact that the dynamics driving chiral symmetry breaking must be imposed by hand via IR boundary conditions. Its shortcomings however include a glueball spectrum that does not fit well the lattice data, the fact that magnetic quarks are confined instead of screened, and asymptotic Regge trajectories for glueballs and mesons are quadratic instead of linear.

2 Improved Holographic QCD

In [9] an improved holographic phenomenological model for QCD was proposed. It reunited inputs from both gauge theory and string theory while keeping the simplicity of a two-derivative action. It could describe both the region of asymptotic freedom as well as the strong IR dynamics of QCD.

The basic fields of the pure gauge theory (the closed string sector) that are non-trivial in the vacuum solution and describe the pure gauge dynamics, are the 5d metric $g_{\mu\nu}$ (dual to the YM stress tensor), a scalar Φ (the dilaton, dual to $Tr[F^2]$) that controls the 't Hooft coupling λ_t of QCD, and an axion a, that is dual to the QCD instanton density $Tr[F\wedge F]$ and its source represents the θ angle. Quarks can be added to the pure gauge theory by adding $D_4-\bar{D}_4$ brane pairs in the background gauge theory solution. The $D_4-\bar{D}_4$ tachyon condensation then induces chiral symmetry breaking, [11,9].

The action for the 5D Einstein-dilaton theory reads,

$$S_5 = M_p^3 N_c^2 \left(-\int d^5x\sqrt{g}\left[R - \frac{4}{3}\frac{(\partial\lambda)^2}{\lambda^2} + V(\lambda)\right] + 2\int_{\partial M} d^4x\sqrt{h}\ K\right) \tag{1}$$

where M_p is the Planck mass. The second term in the action is the Gibbons-Hawking with K being the extrinsic curvature on the boundary.

The only nontrivial input in the two-derivative action of the graviton and the dilaton is the dilaton potential $V(\lambda)$, where $\lambda = e^{\Phi}$. λ is proportional to the 't Hooft coupling of the gauge theory, $\lambda = \kappa\lambda_t$. The constant of proportionality κ is treated as a parameter to be fitted to data. The potential is directly related to the gauge theory β-function once a holographic definition of energy is chosen. Although the shape of $V(\lambda)$ is not fixed without knowledge of the exact gauge theory β-function, its UV and IR asymptotics can be determined.

In the UV, the input comes from perturbative QCD. We demand asymptotic freedom with logarithmic running. This implies in particular that the asymptotic UV geometry is that of AdS_5 with logarithmic corrections. It requires a (weak-coupling) expansion of $V(\lambda)$ of the form $V(\lambda) = 12/\ell^2(1 + v_1\lambda + v_2\lambda^2 + \cdots)$.

Demanding confinement of the color charges restricts the large-λ asymptotics of $V(\lambda)$. In [9] we focused on potentials such that, as $\lambda\to\infty$, $V(\lambda)\sim\lambda^{\frac{4}{3}}(\log\lambda)^{(\alpha-1)/\alpha}$ where α is a positive parameter. The IR asymptotics of the solution in the Einstein frame are:

$$ds_0^2 \to e^{-C\left(\frac{r}{\ell}\right)^{\alpha}}\left(dr^2 + dx_4^2\right), \quad \lambda_0 \to e^{3C/2\left(\frac{r}{\ell}\right)^{\alpha}}\left(\frac{r}{\ell}\right)^{\frac{3}{4}(\alpha-1)} \tag{2}$$

where the constant C is related to Λ_{QCD}. Confinement requires $\alpha \geq 1$. The parameter α characterizes the large excitation asymptotics of the glueball spectrum, $m_n \sim n^{\frac{\alpha-1}{\alpha}}$. For linear confinement, we choose $\alpha = 2$.

The parameters of the holographic model a priori are: the Planck mass M_p, which governs the scale of interactions between the glueballs in the theory, the parameters v_i that specify the shape of the potential, the scale Λ that plays the role of Λ_{QCD} and the AdS scale ℓ. The latter is not a physical parameter but only a choice of scale: only $\Lambda\ell$ enters into the computation of physical observables. Before choosing a potential, κ that relates λ and the 't Hooft coupling, is not a parameter as the physics is independent of κ. This is characteristic of the leading order in the large-N_c expansion. Once a potential has been chosen then it is not the case anymore as κ can be calculated by comparing for example to the perturbative QCD β-function. A specific choice for $V(\lambda)$ was made in [9] with the appropriate asymptotic properties, that only depended on the parameter κ, hence fixing all v_i. Finally, κ and Λ are fixed by matching to the lattice data for the first two 0^{++} glueball masses. Once Λ is fixed, all other interesting scales like the effective QCD string tension σ are also fixed.

Glueball masses can be obtained by computing the spectrum of normalizable fluctuations of the metric and dilaton around the background solution. In table 1 we give an overview of the glueball spectrum calculated here and its comparison to the best existing lattice data both for $N = 3$ and $N \to \infty$. In figure 1 we give the almost linear trajectories of the 0^{++} and the 2^{++} states as computed from our model.

3 Finite temperature and deconfinement

We will now turn to the finite temperature dynamics in the pure gauge sector derived from the setup of[9]. We find that this setup describes very well the basic features of large-N_c Yang Mills at finite temperature. It exhibits a first order deconfining phase transition. The equation of state and speed of sound of the high temperature phase are remarkably similar to the corresponding lattice results. Moreover, using the zero temperature potential and without adding any extra parameter, we obtain a value for the critical temperature in very good agreement with the one computed from the lattice, [10].

The deconfinement transition. At finite temperature there exist two distinct types of solutions to the action (1) with AdS asymptotics:

i. The thermal graviton gas, obtained by compactifying the Euclidean time in the zero temperature solution with $\tau \sim \tau + 1/T$:

$$ds^2 = b_0^2(r)\left(dr^2 + d\tau^2 + dx_3^2\right),\ \lambda = \lambda_0(r).$$

This solution exists for all $T \geq 0$ and it corresponds to the confined phase, if the gauge theory at zero T confines.

ii. The black hole (BH) solutions (in Euclidean time) of the form:

$$ds^2 = b^2(r)\left(\frac{dr^2}{f(r)} + f(r)d\tau^2 + dx_3^2\right),\ \lambda = \lambda(r). \tag{3}$$

with $f(0) = 1$. There exists a singularity in the interior at $r = \infty$ that is now hidden by a regular horizon at $r = r_h$ where f vanishes. Such solutions correspond to a deconfined phase.

As we discuss below, in confining theories the BHs exist only above a certain minimum temperature, $T > T_{min}$.

The thermal gas as well as BH solution has two parameters: T and Λ. Near the horizon, $f \to f_h(r_h - r)$ with $4\pi T = f_h$. From Einstein's equations, [10]:

$$4\pi\, T = b^{-3}(r_h)\left(\int_0^{r_h} \frac{du}{b(u)^3}\right)^{-1}. \tag{4}$$

In the large-N_c limit, the physics is dominated by the saddle point with minimum free energy. For a given temperature we must therefore compare the free energies of solutions i. and ii.

We introduce a cutoff boundary at $r/\ell = \epsilon$ in order to regulate the infinite volume. The difference of the two scale factors is given near the boundary as

$$b(\epsilon) - b_0(\epsilon) = \mathcal{C}(T)\epsilon^3 + \cdots \tag{5}$$

By the standard rules of AdS/CFT we can relate $\mathcal{C}(T)$ to the difference of VEVs of the gluon condensate: $\mathcal{C}(T) \propto \langle \mathrm{Tr} F^2 \rangle_T - \langle \mathrm{Tr} F^2 \rangle_0$.

The free energy difference is given by

$$\frac{\mathcal{F}}{M_p^3 N_c^2 V_3} = 12\frac{\mathcal{C}(T)}{\ell} - \pi T b^3(r_h) = 12\frac{\mathcal{C}(T)}{\ell} - \frac{TS}{4M_p^3 N_c^2 V_3}, \tag{6}$$

where, in the last equality, we used the fact that the entropy is given by the area of the horizon. It is clear that the existence of a non-trivial deconfinement phase transition is driven by a non-zero value for the thermal gluon condensate $\mathcal{C}(T)$.

For a general potential we can prove the following (under mild assumptions):

i. *There exists a phase transition at finite T, if and only if the zero-T theory confines.*

ii. *This transition is of the first order for all of the confining geometries, with a single exception described in iii:*

iii. *In the limit confining geometry $b_0(r) \to \exp(-Cr)$ (as $r \to \infty$), the phase transition is of the second order and happens at $T = 3C/4\pi$.*

iv. *All of the non-confining geometries at zero T are always in the black hole phase at finite T. They exhibit a second order phase transition at $T = 0^+$.*

We illustrate the function $T(r_h)$ schematically in figure 2. It follows that in the confining geometries $\alpha > 1$, for a given $T > T_{min}$, there always exist a big and a small black hole solution. The big BH has positive specific heat hence it is thermodynamically stable, whereas the small BH is unstable. In the borderline confining geometry $\alpha = 1$, there is a single BH solution.

Existence of a $T_c \geq T_{min}$ follows from the physical requirement of positive entropy. From the first law of thermodynamics, it follows that $d\mathcal{F}/dr_h = -S\, dT/dr_h$. Since $S > 0$ for any physical system, extrema of $\mathcal{F}(r_h)$ coincide with the extrema of $T(r_h)$. Using also the fact that $\mathcal{F}(r_h) \to -\infty$ for $r_h \to 0$ and $\mathcal{F}(r_h) \to 0$ near $r_h \to \infty$, we arrive at conclusion (ii) described above: *There is a first order transition for all of the confining geometries* (This becomes second order for the borderline case $\alpha = 1$).

The small r_h asymptotics also allows us to fix the value of the Planck mass in (1). This geometry corresponds to an ideal gas of gluons with a free energy density (We use lowercase letters for the densities of the corresponding functions) $f \to (\pi^2/45)N_c^2 T^4$. As the geometry becomes AdS, eq. (6) implies that: $f \to \pi^4 (M_p \ell)^3 N_c^2 T^4$. We conclude that $M_p \ell = \left(45\pi^2\right)^{-\frac{1}{3}}$. Using the value of ℓ in [9], we obtain $M_p \approx 2.3$ GeV.

4 Numerical Results at finite temperature

In [9] an explicit form of the scalar potential with the correct asymptotics was proposed. The resulting background, that corresponds to the choice $\alpha = 2$ in (2), exhibits asymptotic freedom, linear confinement, and a glueball spectrum in very good quantitative agreement with the lattice data. Here we present a numerical computation of the relevant thermodynamic quantities in this same theory. Our general analysis shows that this theory has black hole solutions above a temperature T_{min} and exhibits a first order phase transition at some $T_c > T_{min}$

To analyze the behavior of the theory at finite temperature, we have solved numerically Einstein's equations for the metric and dilaton. The integration constants were fixed as explained

earlier. We find a minimum temperature for the existence of black hole solutions, $T_{min} = 210$ MeV.

Next, we compute the free energy difference between the black hole and thermal gas solutions, as a function of temperature.

The resulting free energy as a function of the temperature is shown in the left of figure 3, which clearly shows the existence of a minimum temperature, and a first order phase transition at $T = T_c$, where $\mathcal{F}(T_c) = 0$. For $T < T_c$, the thermal gas dominates, and the system is in the confined phase. For $T > T_c$, the (large) black hole dominates, corresponding to a deconfined phase. The entire small black hole branch is always thermodynamically disfavored.

The value we obtain for the critical temperature, $T_c = \mathbf{235 \pm 15}$ MeV, is close to the value obtained for large-N Yang-Mills [12], which with our normalization of the lightest glueball would be 260 ± 11 MeV (combining the results in [12] and [13]).

From the free energy we can determine all other quantities by thermodynamic identities:

$$p = -\mathcal{F}/V_3, \quad s = 4\pi M_p^3 N_c^2 b_T^3(r_h), \quad \epsilon = p + Ts. \tag{7}$$

Next, we present some of the thermodynamic quantities that are compared with the lattice results.

`Latent Heat`. The latent heat per unit volume is defined as the jump in the energy at the phase transition, $L_h = T_c \Delta s(T_c)$, and it is expected to scale as N_c^2 in the large N_c limit [12]. From eq. (7) we note that this expectation is reproduced in our theory. Quantitatively, we find $L_h^{1/4}/T_c \simeq 0.65\sqrt{N_c}$. This is to be compared with the value 0.77 reported in [12].

`Equation of state and the trace anomaly.` A useful indication about the thermodynamics of a system is given by the relations between the quantities ϵ/T^4, $3(p/T^4)$, $3/4(s/T^3)$. In the right of figure 3 we compare our results for these quantities with the corresponding lattice results, reported in [14] (for N_c=3). We find good qualitative agreement. In the low temperature phase, the thermodynamic functions vanish to the leading order in N_c^2 and the jump in ϵ and s at T_c reflects the first order phase transition. The fact that our curves lay below the lattice curves may be traced back to the relative smallness of the latent heat in our model.

The *trace anomaly*, $(\epsilon - 3p)/T^4$, is plotted in the left of figure 4, together with the lattice result from [14]. From eq. (6), $\epsilon - 3p \propto \mathcal{C}(T)$, consistent with our interpretation of $\mathcal{C}(T)$ as the gluon condensate.

`Speed of sound.` This quantity is defined as $c_s^2 = (\partial p/\partial \epsilon)_S = s/c_v$. It is expected to be small at the phase transition, and to reach the conformal value $c_s^2 = 1/3$ at high temperatures. In the right of figure 4 we compare our results with the lattice data, finding good agreement.

`Shear viscosity.` In agreement with the general results of [15], the ratio between shear viscosity and entropy density is $\eta/s = (4\pi)^{-1}$.

Acknowledgments

This article is based on the talk presented by E. Kiritsis at this meeting. U. Gursoy and F. Nitti are supported by European Union Individual Marie Curie fellowships MEIF-CT-2006-039962 and -039369. L. Mazzanti is supported by INFN and ICTP fellowships. This work was partly suposrted by ANR grant, ANR-05-BLAN-0079-02, RTN contracts MRTN-CT-2004-005104 and MRTN-CT-2004-503369, CNRS PICS # 2530, 3059 and 3747, and by a European Union Excellence Grant, MEXT-CT-2003-509661.

References

1. S. Dimopoulos and L. Susskind, Nucl. Phys. B **155** (1979) 237.

J^{PC}	[18] (MeV)	This model (MeV)	Mismatch	$N_c \to \infty$ [17]	Mismatch
0^{++}	**1475 (4%)**	**1475**	0	**1475**	0
2^{++}	2150 (5%)	2055	4%	2153 (10%)	5%
0^{-+}	**2250 (4%)**	**2243**	0		
0^{++*}	**2755 (4%)**	**2753**	0	2814 (12%)	2%
2^{++*}	2880 (5%)	2991	4%		
0^{-+*}	3370 (4%)	3288	2%		
0^{++**}	3370 (4%)	3561	5%		
0^{++***}	3990 (5%)	4253	6%		

Table 1: *Comparison between the glueball spectra in Ref. I and in our model. The states we use as input in our fit are marked in bold. The parenthesis in the lattice data indicate the percent accuracy.*

2. P. Anastasopoulos, T. P. T. Dijkstra, E. Kiritsis and A. N. Schellekens, Nucl. Phys. B **759** (2006) 83 [arXiv:hep-th/0605226].
3. G. 't Hooft, *"A planar diagram theory for strong interactions"* Nucl. Phys. B **72** (1974) 461.
4. A. V. Manohar, [ArXiv:hep-ph/9802419].
5. J. M. Maldacena, Adv. Theor. Math. Phys. **2**, 231 (1998) [Int. J. Theor. Phys. **38**, 1113 (1999)]
6. E. Witten, Adv. Theor. Math. Phys. **2** (1998) 505 [ArXiv:hep-th/9803131]; J. M. Maldacena and C. Nunez, Phys. Rev. Lett. **86** (2001) 588 [ArXiv:hep-th/0008001]; I. R. Klebanov and M. J. Strassler, JHEP **0008** (2000) 052 [ArXiv:hep-th/0007191].
7. J. Polchinski and M. J. Strassler, Phys. Rev. Lett. **88** (2002) 031601 [ArXiv:hep-th/0109174]; Phys. Rev. Lett. **88** (2002) 031601 [ArXiv:hep-th/0109174].
8. J. Erlich, E. Katz, D. T. Son and M. A. Stephanov, Phys. Rev. Lett. **95**, 261602 (2005) [arXiv:hep-ph/0501128]; L. Da Rold and A. Pomarol, Nucl. Phys. B **721**, 79 (2005) [ArXiv:hep-ph/0501218].
9. U. Gursoy and E. Kiritsis, JHEP **0802** (2008) 032 [arXiv:0707.1324 [hep-th]]; U. Gursoy, E. Kiritsis and F. Nitti, JHEP **0802** (2008) 019 [arXiv:0707.1349 [hep-th]].
10. U. Gursoy, E. Kiritsis, L. Mazzanti and F. Nitti, arXiv:0804.0899 [hep-th].
11. R. Casero, E. Kiritsis and A. Paredes, Nucl. Phys. B **787** (2007) 98; [ArXiv:hep-th/0702155].
12. B. Lucini, M. Teper and U. Wenger, JHEP **0502**, 033 (2005) [arXiv:hep-lat/0502003].
13. B. Lucini and M. Teper, JHEP **0106**, 050 (2001) [arXiv:hep-lat/0103027].
14. G. Boyd, J. Engels, F. Karsch, E. Laermann, C. Legeland, M. Lutgemeier and B. Petersson, Nucl. Phys. B **469**, 419 (1996) [arXiv:hep-lat/9602007].
15. A. Buchel and J. T. Liu, Phys. Rev. Lett. **93**, 090602 (2004) [arXiv:hep-th/0311175].
16. S. S. Gubser and A. Nellore, arXiv:0804.0434 [hep-th].
17. B. Lucini and M. Teper, *"SU(N) gauge theories in four dimensions: Exploring the approach to N =∞,"* JHEP **0106** (2001) 050 [ArXiv:hep-lat/0103027].
18. H. B. Meyer, *"Glueball Regge trajectories,"* [ArXiv:hep-lat/0508002].

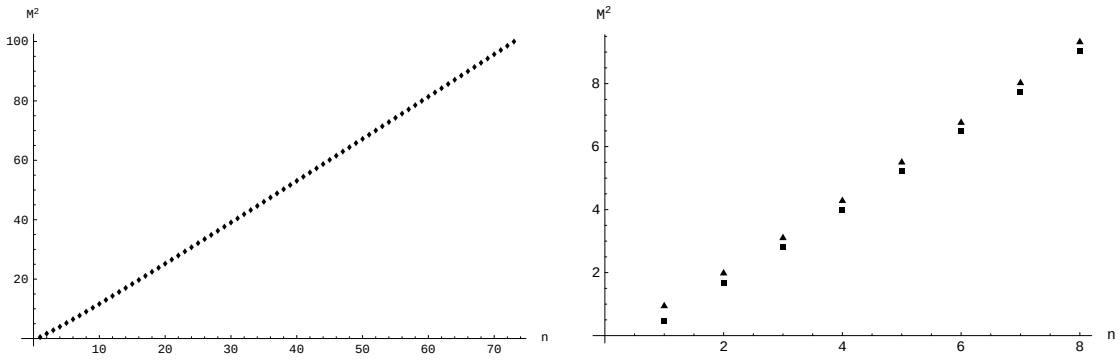

Figure 1: *Left: Linear pattern in the spectrum for the first 40 0^{++} glueball states. M^2 is shown units of $0.015\ell^{-2}$. Right: The first 8 0^{++} (squares) and the 2^{++} (triangles) glueballs. We used $b_0 = 4.2, \lambda_0 = 0.05$.*

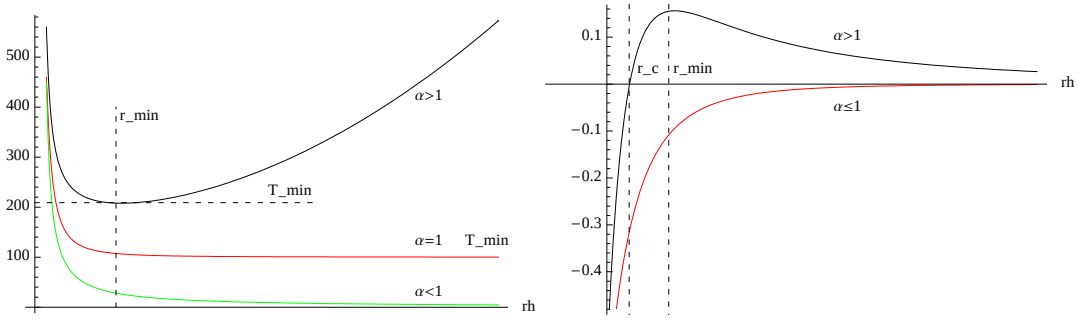

Figure 2: Schematic behavior of temperature as a function of r_h (left) and the free energy density as a function of r_h, (right) for the infinite-r geometries of the type (2), for different values of α.

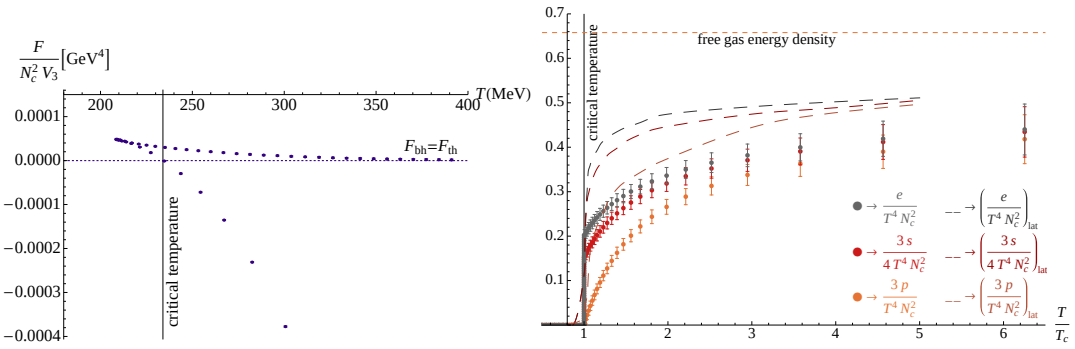

Figure 3: Left: Black hole free energy. Right: Dimensionless thermodynamic functions. The dashed curves correspond to the lattice data of reference [14].

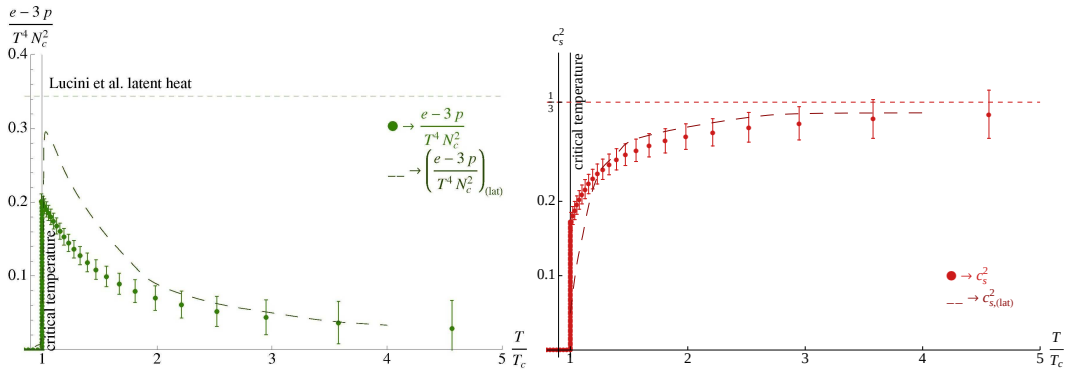

Figure 4: *Left: The trace anomaly. Right: The speed of sound. The dashed curves are the lattice result of reference [14].*